


Designing multifunctional two-dimensional layered transition metal phosphorous chalcogenides

M. J. Swamynadhan¹ and Saurabh Ghosh^{1,2,*}

¹*Department of Physics and Nanotechnology, SRM Institute of Science and Technology, Kattankulathur 603 203, Tamil Nadu, India*

²*SRM Research Institute, SRM Institute of Science and Technology, Kattankulathur 603 203, Tamil Nadu, India*

 (Received 21 November 2020; revised 15 March 2021; accepted 4 May 2021; published 18 May 2021)

Layered two-dimensional (2D) transition metal phosphorous chalcogenides (TMPCs) are now in intense research focus due to their interesting ferroelectric and magnetic properties and compatibility with 2D electronic devices. Here, we have employed first-principles density functional theory calculations to investigate the electric and magnetic properties of ABP_2S_6 ($A = Cu, Ni$; $B = Cr, Mn$) TMPCs. We have systematically investigated four TMPCs compounds, namely, $CuCrP_2S_6$, $CuMnP_2S_6$, $NiCrP_2S_6$, and $NiMnP_2S_6$, and reported unusual antiferroelectric/ferroelectric (AFE/FE) and electronic properties. We have found a more stable ferroelectric state in van der Waals (vdW) gap with higher polarization compared to the usual ferroelectric phase in the insulating state. In case of $CrMnP_2S_6$ and $NiMnP_2S_6$, we have proposed them as polar half-metals as our analysis have revealed that ferroelectric distortions can persist in these systems in the metallic phase. Moreover, our analysis have shown that $NiMnP_2S_6$ can undergo metal-to-insulator transition driven by the polar distortion. We have identified two modes namely, Γ_2^- & Γ_1^+ , those are responsible for driving ferroelectricity and antiferroelectricity, respectively, into these systems. We could observe a rare and interesting phenomena, where the antipolar mode Γ_1^+ that is responsible for antiferroelectric distortion leads to a ferroelectric distortion when applied excessively on the system, which is unusual. Finally, we have performed molecular dynamics simulations at various finite temperatures. In case of $NiCrP_2S_6$ and $NiMnP_2S_6$ at 300 K, we have observed that the ferroelectric state within the vdW gap is stable. Interestingly, we have discovered a hybrid inter-intra layer antiferroelectric configuration within the vdW gap for $CuCrP_2S_6$. The layers start to move opposite to each other due to the temperature effect, which leads to the switching of the AFE state in the first layer. Further, increase of temperature results the switching in both the layers. The reported in-gap FE/AFE states in vdW gap can be tuned by uniaxial strain along the perpendicular direction of the 2D layer and thus the materials studied here can be considered as potential piezoelectric materials.

DOI: [10.1103/PhysRevMaterials.5.054409](https://doi.org/10.1103/PhysRevMaterials.5.054409)

I. INTRODUCTION

The discovery of fascinating new physical phenomena in two-dimensional (2D) materials facilitates exciting multifunctionalities and device concepts for electronics, spintronics, and energy storage devices [1–7]. In particular, 2D multiferroic materials are of special interest where both ferroelectricity and magnetism just not only coexist but also are cross coupled that can lead to applications in spintronic memory and energy harvesting technologies [2,8]. The primary challenge in multiferroics is to identify materials that have a strong coupling between electrical polarization (P) and magnetization (M) at room temperature [9–11]. Further, materials with 2D layered structure with strong P-M coupling is rare compared to the inorganic bulk materials [3–5]. Multiferroic materials in 2D layered form can be efficiently integrated with the present device manufacturing techniques and thus more research is currently being pursued to discover potentially such compositions [12–14]. In this regard, 2D ABP_2S_6 (A and B are transition metals) transition metal phosphorous chalcogenides (TMPCs) are investigated in great details in order to

explore the possibility of multiferroic functionalities [15–17]. In these van der Waals (vdW) layered structures the polarization is originated due to the out of plane displacement of the A sites whereas the transition metals at B sites (Mn, Cr, Co, etc.) give rise to magnetization [18,19]. Considering the ferroelectricity alone, the prototype proper ferroelectric materials like $BaTiO_3$ or $PbTiO_3$ show double-well energy landscape having two stable ferroelectric (FE) (i.e., pol up and pol down) state where the polarization reversal can be demonstrated by the reversal of applied electric field [1,18,20]. Recently, for the first time, $CuInP_2S_6$ was reported to exhibit a quadruple potential well, i.e., there are four stable polarization states, in two situations Cu atoms are at the edge of the 2D plane (low pol up and low pol down) and in the other two situations the Cu atoms are in the van der Waals gap (i.e., high pol up and high pol down) [1]. The magnitude of pol of the new in-gap FE state in van der Waals gap is almost double than the value observed within the layer. Further, these new stable states can be tuned by applying external pressure and electric field. Here, note that $CuInP_2S_6$ is nonmagnetic. [1,20,21].

Considering multiferroic TMPCs, these compounds show considerable coupling between the spin and electric dipole orientation [18,19], although they are found to be originated from different sites (A site for ferroelectricity and B sites for

*saurabhghosh2802@gmail.com

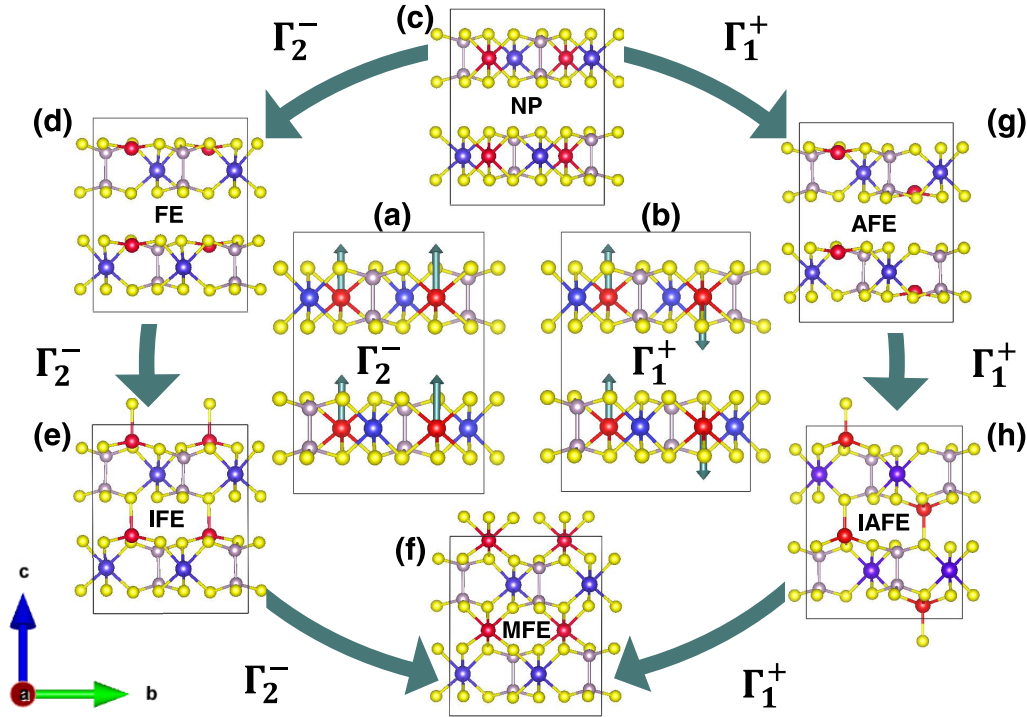


FIG. 1. Functional modes and possible ferroelectric/antiferroelectric configurations in TMPCs. In (a) ferroelectric Γ_2^- mode, (b) antiferroelectric Γ_1^+ mode, (c) nonpolar (NP), (d) ferroelectric (FE), (e) in-gap ferroelectric (IFE), (f) midgap ferroelectric (MFE), (g) antiferroelectric (AFE), and (h) in-gap antiferroelectric (IAFE) configurations are illustrated. The various FE/IFE and AFE/IAFE states have been produced by applying Γ_2^- and Γ_1^+ mode, respectively. The vectors as shown in (a) and (b) indicate the displacements of the A-site cations. The red color balls indicate A-site atoms (Cu/Ni), purple color balls indicate B-site atoms (Cr/Mn), yellow color balls indicate sulphur (S) atoms, and pink color balls indicate phosphorous (P) atoms.

magnetism). However, the P-M coupling is expected to be more stronger if the two properties originated from the same site and that raises a key question. Can the quadruple nature of the polarization be retained if the magnetic elements are considered at A sites in ABP_2S_6 ? In addition, possibility of strong P-M coupling via this route and the associated modifications in the electronic structure (i.e., metal vs insulator) need to be investigated in great detail in the interest of device applications, which leads to the scope of the present paper.

In this paper, we have studied structural, electronic, and magnetic properties of a set of ABP_2S_6 (A=Cu, Ni; B=Cr, Mn) TMPCs in 2D bilayer form by first-principles density functional theory (DFT) calculations. Here, we have considered four compounds, namely, $CuCrP_2S_6$ (CCPS), $CuMnP_2S_6$ (CMPS), $NiCrP_2S_6$ (NCPS), and $NiMnP_2S_6$ (NMPS). In all the ABP_2S_6 compounds the sum of the nominal valence states of A and B sites has to be +4 to maintain the charge neutrality condition as P and S are in nominal valence states of +4 and -2, respectively. In $CuCrP_2S_6$, the Cu atoms at A site are in nominal +1 charge state and Cr atoms at B sites are in nominal +3 charge state. Thus, in terms of 3d-level occupancy Cu is in d^{10} and gives rise to finite polarization while Cr being in d^3 gives rise to finite magnetization. Similarly, in case of $CuMnP_2S_6$, Mn is expected to be in +3 charge state and Cu to be in +1 charge state, but our calculations have suggested that Mn becomes +2 and thus forces Cu to be also in +2 state. Here, magnetization is originating from partially filled d electrons with $3d^5$ and $3d^1$ occupancies of

Mn and Cu, respectively. In case of $NiCrP_2S_6$ and $NiMnP_2S_6$, Ni at A site is in +2 charge state, i.e., $3d^8$ nominal electronic occupancy. Due to +2 charge state of Ni, Cr and Mn at B sites are forced to be in +2 charge state with $3d^4$ and $3d^5$ respective occupancies.

We have reported that these layered materials are energetically stable and simultaneously possess electric and magnetic properties. The electric dipole moment is found to be originating from Cu/Ni displacement along the axis perpendicular to the layer plane. In case of $NiBP_2S_6$ systems where B = Cr or Mn, additional magnetic interactions between Ni and Cr or Mn (at B site) ions are now possible that could lead to rich P-M phase diagram. We have constructed various possible antiferroelectric/ferroelectric structural phases produced by structural modes along the c axis governed by the symmetry. They are namely, nonpolar (NP), ferroelectric (FE), antiferroelectric (AFE), in-gap ferroelectric (IFE), in-gap antiferroelectric (IAFE), and midgap ferroelectric (MFE) configurations as shown in Fig. 1(a)–1(f) (see Fig. S1 within the Supplemental Material [22] for top view—along c axis). All possible magnetic interactions have been considered within the mentioned structural phases. We have discussed the recipe of strong coupling between polarization, magnetization, and electronic structure (metal-to-insulator transition) in this family of materials. Finally, to capture the structural changes and its effect on the properties, we have performed finite-temperature molecular dynamics (MD) simulations. The MD simulations revealed a hybrid inter-intra layer

TABLE I. Properties of the four compounds, namely, CuCrP_2S_6 (CCPS), CuMnP_2S_6 (CMPS), NiCrP_2S_6 (NCPS), and NiMnP_2S_6 (NMPS) studied in this paper. Abbreviations are FM: ferromagnetic; FiM: ferrimagnetic; NP: nonpolar; FE: ferroelectric; AFE: antiferroelectric; IFE: in-gap ferroelectric; IAFE: in-gap antiferroelectric; MFE: midgap ferroelectric.

System	Electronic property	Magnetic ordering	Stable states	Polarization along the c axis ($\mu\text{C}/\text{cm}^2$)
CuCrP_2S_6	Insulating	FM	NP, FE, AFE, IFE and IAFE	FE = 11.08, IFE = 16.36
CuMnP_2S_6	Metallic	FiM	NP, FE, IFE	
NiCrP_2S_6	Insulating	FiM	NP, IFE	IFE = 3.93
NiMnP_2S_6	Insulating-to-Metallic	FiM	NP, IFE, MFE	FE = 9.28

antiferroelectric configuration with usual antiferroelectric switching.

II. COMPUTATIONAL DETAILS

Density functional theory (DFT) [23] calculations have been performed using the Vienna *ab initio* simulation package (VASP) [24] within the choice of projector augmented waves (PAW) basis set [25]. The Perdew-Burke-Ernzerh (PBE) functional has been used to treat the exchange and correlation functional [26]. The cutoff energy is set as 500 eV. All the structures have been fully relaxed until all forces on every atoms are smaller than $0.001 \text{ eV}/\text{\AA}$. A dense k-point mesh of $11 \times 7 \times 5$ has been used for 2D layered bulk materials. The additional effective Hubbard U parameter U_{eff} (U-J_H) has been adopted for Cr, Mn, and Ni atoms with values of values as 3.0 eV, 4.0 eV, and 6.0 eV, respectively. In case of MD simulations, the Brillouin zone has been sampled only at the Γ point. The canonical ensemble (NVT) by the Nose-Hoover approach [27] has been used [28,29] with a plane wave-basis cut-off energy of 500 eV with 5-fs time interval (time steps) between MD steps. To see how the displacement vs energetic curve depend on van der Waals (vdW) correction, we perform calculations using Grimme's zero damping method [30,31] and Becke-Jonson damping method [31]. While comparing the optimized cell parameters with the experimentally reported values, our calculation without vdW correction gives $\sim 1.06\%$ error especially in c parameter, while DFT-D3 (BJ) vdW method gives $\sim 5.2\%$ and DFT-D3 (Grimme) vdW method gives $\sim 3.1\%$ error in the optimized c parameter. We have compared the results with and without vdW corrections at each section. We observed some changes in the energy barriers, which are enhanced by the inclusion of vdW corrections. The main results presented and the outcome inferred from it remain unchanged. The results obtained with the vdW correction are the same with a strained (along the c axis) situation without the correction. Hence, most of our discussions are based on the without vdW correction calculations. However, in each section we have included the results with and without vdW correction and discuss accordingly.

The AMPLIMODES (symmetry mode analysis) [32] and PSEUDO [33] (a program for pseudosymmetry search) have been used to understand the structural modes involved in the phase transition.

III. RESULTS AND DISCUSSION

The CuCrP_2S_6 is a van der Waals layered material with lattice constants $a = 5.9 \text{ \AA}$; $b = 10.3 \text{ \AA}$; $\alpha, \gamma = 90^\circ$; $\beta =$

104.8° (see Table I within Supplemental Material [22] for more details). Considering a particular monolayer, each edge of the monolayer consists of a group of six S atoms and two P atoms and the Cr and Cu atoms are situated at the middle the two edges, i.e., at the center of symmetry. The thickness of each monolayer is 2.6 \AA and monolayers are stacked along the c axis with a 3.4 \AA van der Waals gap. In Fig. 1(a), we have shown the polar Γ_2^- mode responsible for ferroelectricity. This particular mode is originating due to the off centring of the A site from center of symmetry along the c axis. On the other hand, in Fig. 1(b), we have shown the antipolar Γ_1^+ mode responsible for antiferroelectricity. Interestingly, in this class of materials due to the geometry and possible relative positions of A atoms within the vdW gap, other forms of ferroelectric and antiferroelectric phases are possible. The NP configuration has been shown in Fig. 1(c). The FE, in-gap FE (IFE), and midgap ferroelectric (MFE) states can be constructed by the application of Γ_2^- mode starting from the NP state, as shown in Figs. 1(d), 1(e), and 1(f), respectively. Similarly, Γ_1^+ mode [Fig. 1(b)] that drives the adjacent A site atoms in antiparallel alignment along the c direction can also lead to the same MFE state starting from NP via the AFE and in-gap antiferroelectric (IAFE) states, as shown in Figs. 1(g) and 1(h), respectively. It is fascinating and a rare phenomena where a antipolar mode driving a system in antiferroelectric states finally leading to a polar MFE state. In other words both Γ_2^- and Γ_1^+ drive the system to a polar state MFE when added extensively. In the following sections we have discussed the stability and functionality of the modes at various FE and AFE configurations.

A. Properties of CuCrP_2S_6

We first discuss the CuCrP_2S_6 (CCPS) compound, which is known to be an antiferroelectric experimentally [34–36]. Previous reports showed a stable FE state of CCPS can only be achieved by the application of an electric field [18]. Here, we have started with a stable NP state where both Cu and Cr atoms are in the middle of the monolayer producing no polarization as shown in Fig. 1(c). When the polar distortion mode Γ_2^- has been applied on the Cu atoms along the +ve c axis, we have obtained a stable FE state at an equilibrium distortion of $\sim 1.3 \text{ \AA}$, where the Cu atoms are shifted at the edge of their respective monolayers [see Fig. 1(d)]. We have found that the FE state is energetically more stable than NP. The net polarization produced due to this polar distortion is $11.08 \mu\text{C}/\text{cm}^2$. The polarization here is similar to few uniaxial transition-metal oxide ferroelectrics having the range of 11 to $71 \mu\text{C}/\text{cm}^2$ [37]. Although it is noteworthy that polarization of $11.08 \mu\text{C}/\text{cm}^2$ is fairly larger than

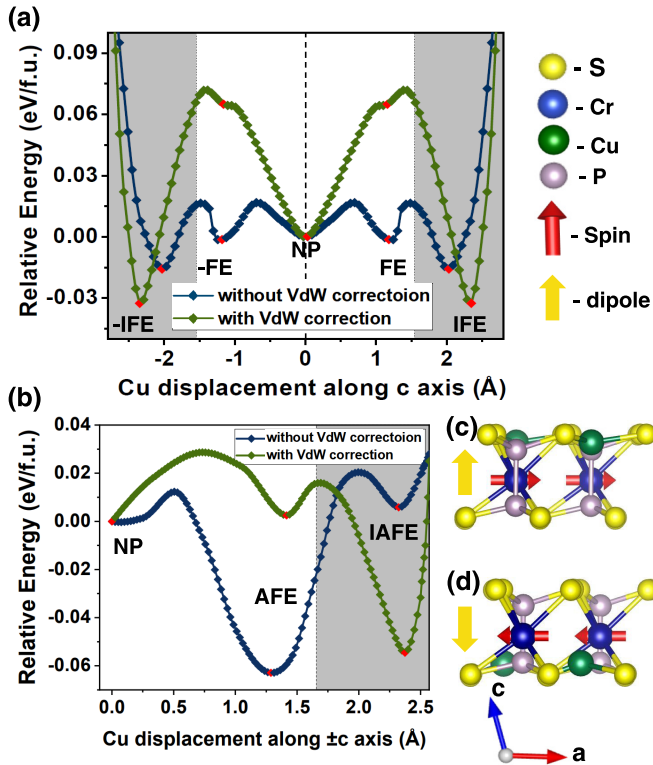


FIG. 2. Ferroelectric/antiferroelectric property of CuCrP_2S_6 (CCPS). In (a) and (b) change in energy (per f.u.) vs the mode amplitude (Q) along the c axis for ferroelectric Γ_2^- (FE) mode and Γ_1^+ (AFE) mode, respectively, has been shown. The grey shaded areas indicate the van der Waals gap. In (c) and (d) magnetization reversal due to polarization switching has been illustrated. Blue/red arrow indicates the polarization direction/easy magnetization direction for two FE states. Blue and green lines indicate with and without vdW correction, respectively. Yellow, pink, blue, and green balls indicate S, P, Cr, and Cu atoms, respectively.

the previously reported values of polarization in some of the ferroelectric materials, having spontaneous polarization $< 1 \mu\text{C}/\text{cm}^2$. Especially, in $(\text{NH}_4)_2\text{SO}_4$, the spontaneous polarization value is $0.62 \mu\text{C}/\text{cm}^2$, some rare earth (R) magnetites like RMnO_3 have polarization in the order of $2.5 \mu\text{C}/\text{cm}^2$ [38]. The CuInP_2S_6 that is similar kind of van der Waals 2D layered material is found to have polarization of the order of $4.93 \mu\text{C}/\text{cm}^2$ [1].

In the next step, we have further displaced the Cu atoms beyond the edge of the monolayer building block into the van der Waals gap by applying the same Γ_2^- mode. The system has achieved a IFE state more stable than the previous NP and FE states through the displacement of Cu atoms $\sim 2 \text{ \AA}$ from its NP position and the system is 0.015 eV/f.u. lower in energy than FE state. The calculated potential barrier between FE and IFE is around $\sim 0.017 \text{ eV/f.u.}$ as shown in the potential energy vs Cu displacement plot in Fig. 2(a) (blue line). The magnitude of the polarization in this IFE state is found to be $16.36 \mu\text{C}/\text{cm}^2$, which is $\sim 47.5\%$ higher than the polarization of FE state. We have shown the difference in the potential energy when vdW corrections are included 2(a) (green line). As discussed in the computational details section,

the c parameter of CCPS is reduced by the vdW corrections. As a result of that, the vdW gap between the layers reduces, which in turn makes the IFE state more stable and FE state less stable. In other words, the vdW correction applies an uniaxial strain along the c axis that tunes the stability of the FE states. Here, these materials studied here can be considered as potential candidate materials for piezoelectric applications.

On the other hand, when we have applied the Γ_1^+ mode the system has found to be in a stable AFE state as shown in Fig. 1(g). This AFE state is more stable than NP and FE states, with energy difference of 0.08 eV/f.u. lower than FE and 0.14 eV/f.u. lower than NP state, respectively. We have further applied the Γ_1^+ mode and we have arrived a local minima when the Cu atoms are in the van der Waals gap. We refer this state as IAFE. The potential energy curve for the antiferroelectric distortion from NP state is shown in Fig. 2(b), blue and green lines indicate with and without vdW corrections, respectively. Here, again the vdW correction produces an uniaxial strain along c axis tuning the stability of the AFE and IAFE states. Here, we would like to point out that as shown in Fig. 2(a) for FE configuration, there is a strong difference in energy in the van der Waals region between the two cases (vdW vs non-vdW). However, as shown in Fig. 2(b) for AFE case, the difference between vdW and non-vdW is very strong in both regions. We have utilized the DFT-D3 method as implemented in VASP to consider the van der Waals interactions in the systems. We note that this method takes account of the local geometry [30,31]. As shown in Figs. 1(c)–1(e), the optimized geometry varies as we transition from NP to IFE to AFE phases. There are significant displacements between the A-site and B-site atoms with respect to the sulfur and phosphorus atoms. This is reflected in our results as represented in Figs. 2(a) and 2(b) and may be the possible explanation for the discrepancy. However, more detailed study is required in this context with various implementations of van der Waals corrections, which is not within the scope of the present paper.

The climbing-image nudged elastic band calculation (CI-NEB) reveals the energy barrier for the lowest energy path from AFE to FE is around 0.2 eV/f.u. and from FE to AFE state is around 0.11 eV/f.u. (see Fig. S2 within the Supplemental Material [22]). This energy barrier of 0.2 eV/f.u. can be overcome with the help of external electric field [19]. Hence, producing FE state from a stable AFE state may be achieved by the application of an electric field while at the same time $\sim 0.11 \text{ eV}$ barrier between FE and AFE prevents FE state from de-exciting to the AFE state in the absence of an electric field. The partial density of states (PDOS) plots and the electronic band structure indicate the appreciable difference in the band gaps of these states (see Fig. S3 within the Supplemental Material [22]). All the five states NP, FE, IFE, AFE, and IAFE are found to be semiconducting with indirect band gaps $0.55, 1.16, 0.86, 0.9,$ and 0.9 eV , respectively. Hence, electric field can be applied to CCPS to tune the ferroelectric and or antiferroelectric property of the material.

The magnetic ground state of CCPS is ferromagnetic (FM) in all the distorted (FE, AFE, IFE, and IAFE) and NP states with $3\mu_B/\text{f.u.}$ total magnetic moment (for local induced magnetic moment see Table I within the Supplemental Material [22]). The FM state is 0.010 eV/f.u. lower in energy than

the antiferromagnetic (AFM) state. To know the easy magnetization direction, we have performed noncollinear magnetic calculation with spin orbit coupling. The results reveal that in-plane magnetic spin orientations are lower than out-of-plane orientation. The magnetic anisotropy energy (MAE) for out-of-plane magnetization is $\Delta\text{MAE} = E_c - E_a = 12.8 \mu\text{eV}$. In particular, the $\Delta\text{MAE} = E_{-a} - E_{+a} < 0$ for FE state when the polarization is along $+c$ axis. And when the polarization is switched to $-c$ axis, $\Delta\text{MAE} = E_{-a} - E_{+a} > 0$, which indicates that there exist a strong coupling between polarization axis and easy magnetization axis as shown in Figs. 2(c) and 2(d). These MAE values are higher than that of well known room temperature magnetic Ni, Fe, and Co crystal with MAE around $1 \mu\text{eV}$ [39]. Thus, 2D layered CCPS can be considered as potential magnetoelectric material.

B. Properties of CuMnP_2S_6

The CCPS has been experimentally synthesised and its functionality has already been demonstrated. Now, we have replaced Cr atoms by Mn in CCPS and constructed CuMnP_2S_6 (CMPS) to explore how the properties can be tuned with d -level occupancy. In case of CMPS, we have found both NP and FE (with polar mode amplitude $Q_{FE} = 1.3 \text{ \AA}$) states are stable but FE state is energetically higher than the NP state with a transition barrier of $\sim 0.25 \text{ eV/f.u.}$ (see Fig. S4 within the Supplemental Material [22]). We have further displaced the Cu atom towards the van der Waals gap by applying Γ_2^- mode ($Q_{FE} = 2.4 \text{ \AA}$) and discovered a stable IFE state which is 0.18 eV/f.u. higher than NP state although 0.07 eV/f.u. lower than FE state. In other words this IFE is more stable than FE. The potential barrier from NP to IFE is around 0.27 eV/f.u. and the barrier from IFE to NP is around 0.095 eV/f.u. , which makes the IFE state in CMPS more stable than the IFE observed in CCPS. On the other hand, when we have applied the Γ_1^+ mode on NP state, we have reached a local minima where the Cu atoms are in AFE state [as illustrated in Fig. 1(g)]. This AFE state is 0.17 eV/f.u. higher in energy than the NP state.

The magnetic ground state of all the three (NP, FE, and IFE) states are ferrimagnetic, where Mn atoms are in $+2$ charge state with 5 unpaired d electrons, which give rise to $\sim 5 \mu_B/\text{Mn}$ (DFT calculated value $4.3 \mu_B/\text{Mn}$, see Table I within the Supplemental Material [22] for more details) and Cu in $+2$ charge state with 1 unpaired d electron giving small magnetic moment $< 1 \mu_B/\text{Cu}$ is aligned in the opposite direction to Mn spin. Thus, the spins of Mn and Cu sublattices are coupled antiferromagnetically. The magnetic anisotropy energies (MAE) for out-of-plane magnetization is $\Delta\text{MAE} = E_c - E_b = 19.6 \mu\text{eV}$. Hence, the easy magnetization axis is found to be in along $-b$ axis (i.e., $\Delta\text{MAE} = E_{-b} - E_{+b} < 0$) when the polarization is along $+c$ axis and magnetization axis switches to $+b$ axis when the polarization switches to $-c$ axis (i.e., $\Delta\text{MAE} = E_{-b} - E_{+b} > 0$).

The electronic structure of all three states (NP, FE, and IFE) indicate half-metallic property (see Fig. S5 within the Supplemental Material [22]). Thus, CMPS can be a potential layered polar metal. In this context, we would like to recall that finite polarization can only be measured when a ferroelectric material is in insulating state. As the free electrons

in a metal screen the local electric dipole moments, they prevent the formation of long-range dipole ordering [40]. Hence, in general the coexistence of ferroelectricity and metallicity are mutually exclusive [2]. However, in 1965, Anderson and Blount first suggested that a ferroelectric distortion can also persist in a metal [41]. Recent experimental observation has confirmed the ferroelectric structural transition in a metallic oxide, namely, LiOsO_3 [42]. Moreover, the band gaps of these polar metals can be opened and tuned by controlled intermixing of different elements of the material [43]. In case of CMPS, we have found that the compound is IFE with finite MAE in the half-metallic state which is rare [44–46].

C. Properties of NiCrP_2S_6

In case of CCPS and CMPS, Cu atoms are in A sites and thus give rise to ferroelectric/ferroelectric like (as for the later case the system is metallic) distortion. Here, note that Cu atoms are in d^{10} electronic configuration and thus do not induce magnetic property in the system. To investigate the effect of the partially filled d electrons at A site on the ferroelectric property we have replaced Cu by Ni in CCPS. In NiCrP_2S_6 (NCPS), we found a stable NP state where the A-site Ni atoms are at the middle of the layer. We have applied the polar distortion mode Γ_2^- but we could not find any stable FE state till the sulfur boundaries.

On the other hand, when the adjacent Ni atoms have been moved in antiparallel direction by applying Γ_1^+ mode, the system has achieved a stable AFE state with energy $\sim 0.7 \text{ eV/f.u.}$ higher than the NP state. However, we have found a stable IFE (inter planar FE state in van der Waals gap) with energy 0.22 eV/f.u. higher than the NP state as shown in Fig. 3(b) (blue line). The transition barrier between the NP and IFE state is $\sim 0.45 \text{ eV/f.u.}$ and the barrier from IFE to NP state is $\sim 0.18 \text{ eV/f.u.}$, which is a high barrier to overcome by reasonable thermal perturbations, making the system highly stable. Figure 3(b) (green line) indicates the transition barrier with vdW correction, here the correction further reduces the energy of IFE state while the barrier height is almost the same.

The PDOS plots in Fig. 3(a) and electronic band structure (see Fig. S6 within the Supplemental Material [22]) indicate that the NP and IFE states are semiconducting with indirect band gap 0.50 eV and 0.85 eV , respectively. The polarization in the IFE state produced along c axis due to Ni displacement is calculated to be $3.93 \mu\text{C}/\text{cm}^2$. The magnetic ground state of both NP and IFE states are ferrimagnetic with total magnetic moment of $3 \mu_B$ per TM atom, where Cr atoms are in $+2$ charge state with 4 unpaired d electrons giving $4 \mu_B$ magnetic moment aligned opposite to Ni atoms which are in $+2$ charge state, giving rise to $1 \mu_B$ magnetic moment. Similar to the CMPS, here also we have observed reversal of magnetic anisotropy axis with the reversal of the polarization vector.

D. Properties of NiMnP_2S_6

As discussed in previous sections, we have found that CMPS is a IFE polar metal whereas NCPS is a IFE insulator. This observation leads to a key question, can we expect a metal-to-insulator transition (MIT) if we replace Cu by Ni and Cr by Mn in CCPS leading to the system NiMnP_2S_6 (NMPS)?

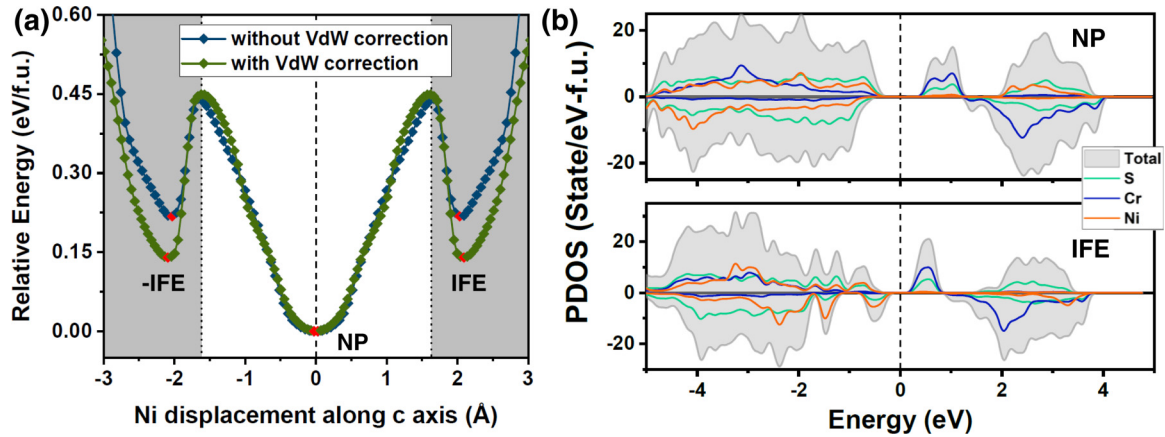


FIG. 3. Ferroelectric and electronic properties of NiCrP₂S₆ (NCPS). In (a) change in the relative energy (per f.u.) vs the mode amplitude (Q) along the c axis for ferroelectric Γ_2^- (FE) mode (blue and green lines indicate with and without vdW correction, respectively) and (b) density of states (DOS) of NP and IFE states are shown. The Fermi energy is set at zero. Here, the grey shaded areas in (a) indicate the van der Waals gap.

We have found that NP state of NMPS is an indirect band-gap insulator with 0.75 eV band gap as shown in Fig. 4(a) (see Fig. S7 within the Supplemental Material [22] for band structure). We have applied the polar distortion in the NP state and found that the band gap reduces gradually leading to a metal-to-insulator transition at $Q_{FE} = 0.69 \text{ \AA}$ from its nonpolar position (middle layer). The polarization values have been calculated for each frozen structure until the metallic state is reached as shown in Fig. 4(b). The polarization has also found to be varying linearly with the polar distortion and reaches a value around $9.28 \mu\text{C}/\text{cm}^2$ before attaining the metallic state.

We have further displaced the Ni atom into the van der Waals gap and found two stable minima. In the first situation, Ni atoms are at the vicinity of the van der Waals gap, which we have defined as IFE in the earlier discussions [also illustrated in Fig. 1(e)]. The second one, where the Ni atoms are found to be in the mid position of van der Waals gap, we have defined this state as MFE [illustrated in Fig. 1(f)]. This MFE state can be achieved by employing maximum distortion of the polar

distortion (irrp. Γ_2^+ , $Q_{FE} = 3.0$). The IFE and MFE states are ~ 0.78 and ~ 0.68 eV/f.u. higher in energy than the NP states, respectively. The barrier from IFE to MFE is found to be 0.1 eV/f.u., which is sufficient enough to separate the states and make them distinguishable as shown in Fig. 5. Note that both the IFE and MFE states are metallic.

The energy barrier for Ni atoms to cross the van der Waals gap is 0.1 eV/f.u. (as shown in Fig. 5) (with and without vdW correction). In other words, the polarization switching between between IFE and MFE can be achieved by crossing the van der Waals gap which is more realistic than crossing the huge barrier across the NP state to switch the FE polarization. In a combined experimental and theoretical study, Neumayer *et al.* [20] have demonstrated that a barrier of ~ 0.8 eV can be crossed by the Cu atom across the van der Waals gap for switching from high polarization state in +c direction (+HP) to high polarization in -c direction (-HP) of the adjacent layer in CrInP₂S₆ by applying external electric field in the order of 1.0 V/Å along the c direction. Hence, crossing a barrier of

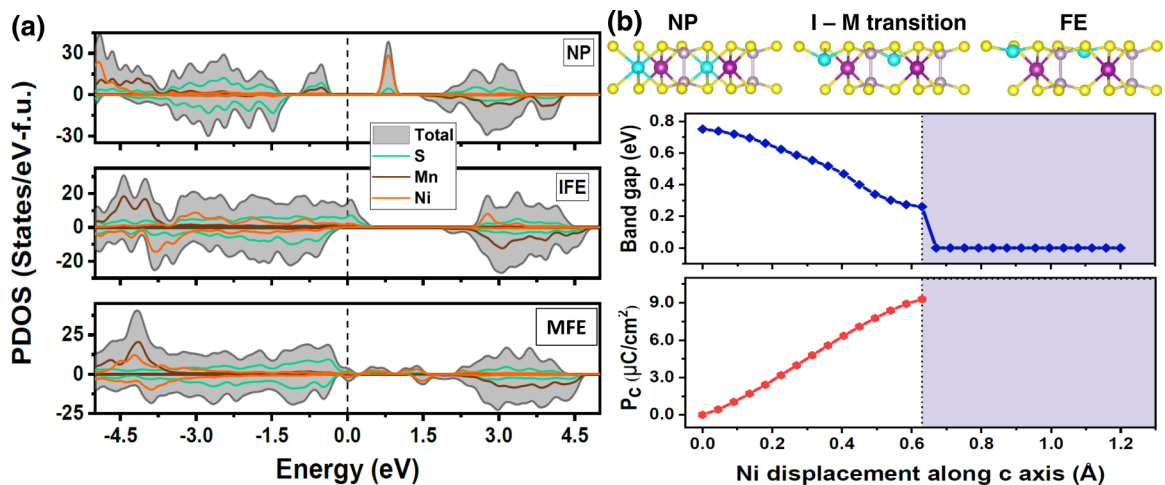


FIG. 4. Electronic property of NiMnP₂S₆ (NMPS). (a) Density of states (DOS) for NP, IFE, and MFE states and (b) variation of band gap (in eV) and polarization (in $\mu\text{C}/\text{cm}^2$) as a function of ferroelectric distortion (Q_{FE}) along the c axis. Grey shaded areas in (b) indicate the van der Waals gap.

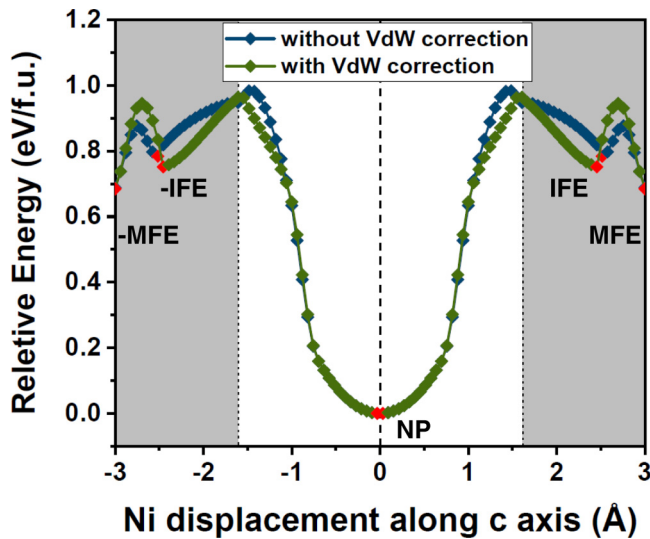


FIG. 5. Ferroelectric property of NiMnP_2S_6 (NMPS). (a) Change in energy (per f.u.) vs the mode amplitude (Q) along the c axis for ferroelectric Γ_2^- (FE) mode. The grey shaded areas indicate the van der Waals gap. The in-gap ferroelectric and midgap ferroelectric states are abbreviated as IFE and MFE, respectively (blue and green lines indicate with and without vdW correction, respectively).

0.1 eV/f.u. in our case can be possible. The low switching barrier across the van der Waals gap makes this compound an effective candidate for magnetic polar metal. On the other hand, a stable AFE state has been obtained through the Γ_1^+ mode. The energy of this AFE state is 0.13 eV/f.u. higher than the NP state, which may make the state difficult to achieve experimentally.

The ground state of NP, FE, IFE, and MFE states are ferromagnetic where Mn (magnetic moment, $4.3 \mu_B$) and Ni spins (magnetic moment, $1.5 \mu_B$) are aligned antiferromagnetically. Further, the noncollinear magnetic calculation at these states indicates the easy magnetization is in the ab plane ($\Delta\text{MAE} = E_c - E_b \sim 0.05 \text{ meV/f.u.}$) and a strong coupling between the direction of polarization and the easy magnetization direction can be observed. Thus, the NMPS system can be considered as a potential candidate where the ferroelectric mode can tune the both the electronic and magnetic property of the system displaying strong coupling between structural, electronic, and magnetic degrees of freedom.

E. Finite-temperature analysis through quantum molecular dynamics (QMD) simulations

To understand the behavior and stability of the systems at finite temperatures, we have performed QMD calculations at various temperatures (100 K, 300 K, and 600 K). First, we have studied the CCPS system for 50 ps at 100 K, 300 K, and 600 K. At time $t = 0$ as initial configuration, we have considered NP state where all the four Cu atoms are at the centrosymmetric position within the layer. At 100 K, the Cu atoms have quickly moved to the AFE state and remained at that state during the molecular dynamics simulation time. Also, except Cu atoms all the other atoms are found to be almost stationary about their mean positions (see Fig. S8 within the Supplemental Material [22]).

Interestingly, at 300 K we have observed switching between two possible intra-antiferroelectric states as shown in Fig. 6(a) and leads to configuration which we have defined as hybrid inter-intra layer antiferroelectric coupling. The trajectories of the atoms are shown in Figs. 6(b) and 6(c) projected on the bc and ac plane, respectively. In Fig. 6(d), we have shown the snapshots of the configurations before, during and after the switching as marked by states F1, F2, and F3, respectively. Our analysis have revealed that finite-temperature effect induces relative displacement between the layers in the opposite direction along b crystallographic axis, as a result of that, the Cu atoms in the first layer experience a force which in turn displaces them in the opposite direction along c . This leads to the transition $F1 \Rightarrow F2 \Rightarrow F3$ [Fig. 6(d)]. On the other hand, this type of layer sliding could not be observed in the system optimized with vdW correction. The reason is, since our MD calculations are at finite volume (NVT—canonical ensemble) the vdW corrected optimized system experiences an uniaxial strain along c axis, which makes the IFE states very stable and the bond between the layers are strong enough to restrict the relative displacement of the layers. However, the same AFE switching is observed in the system with the vdW correction but at different time scale (see Fig. S10 within the Supplemental Material [22]). This indicates that our prediction of switching between AFE states as a result of temperature is valid. Both with and without van der Waals corrections produces same results at different strain conditions. Further, at 600 K, frequent switching has been observed in both the layers (see Fig. S9 within the Supplemental Material [22]). This type of temperature-dependent antiferroelectric switching is unusual and can be of fundamental use in memory related devices. In case of CMPS, NCPS, and NMPS, the respective potentials barriers are large enough that the states may not be switched with thermal fluctuations. However, they can be achieved by applying electric field [20]. We have performed the molecular dynamics calculations at 300 K to assure the stability of IFE state of NCPS and MFE state of NMPS. The trajectories of these systems are given in Supplemental Material [22] (see Figs. S11 and S12), which proves that these states are highly stable when once the state is achieved by applying temperature or electric field.

IV. CONCLUSION

Using first-principles density functional theory calculations guided by group theory, we have investigated a set of 2D layered multiferroic transition metal phosphorous chalcogenides. The summary of our results has been tabulated in Table I. First, we have identified two modes namely, Γ_2^- and Γ_1^+ those are responsible for driving ferroelectricity and antiferroelectricity, respectively, into these systems. We observed a rare and interesting phenomena, where the antipolar mode Γ_1^+ , which is responsible for antiferroelectric distortion leads to a ferroelectric distortion midgap ferroelectric (MFE) when applied excessively on the system; such distortions can be studied further for more interesting and deep understanding, which can lead to a new type of ferroelectricity. Employing Γ_2^- mode, we have found a penta-well landscape for CuCrP_2S_6 with one zero-polarization (NP) state and two finite-polarization states (FE and IFE) on the either sides of

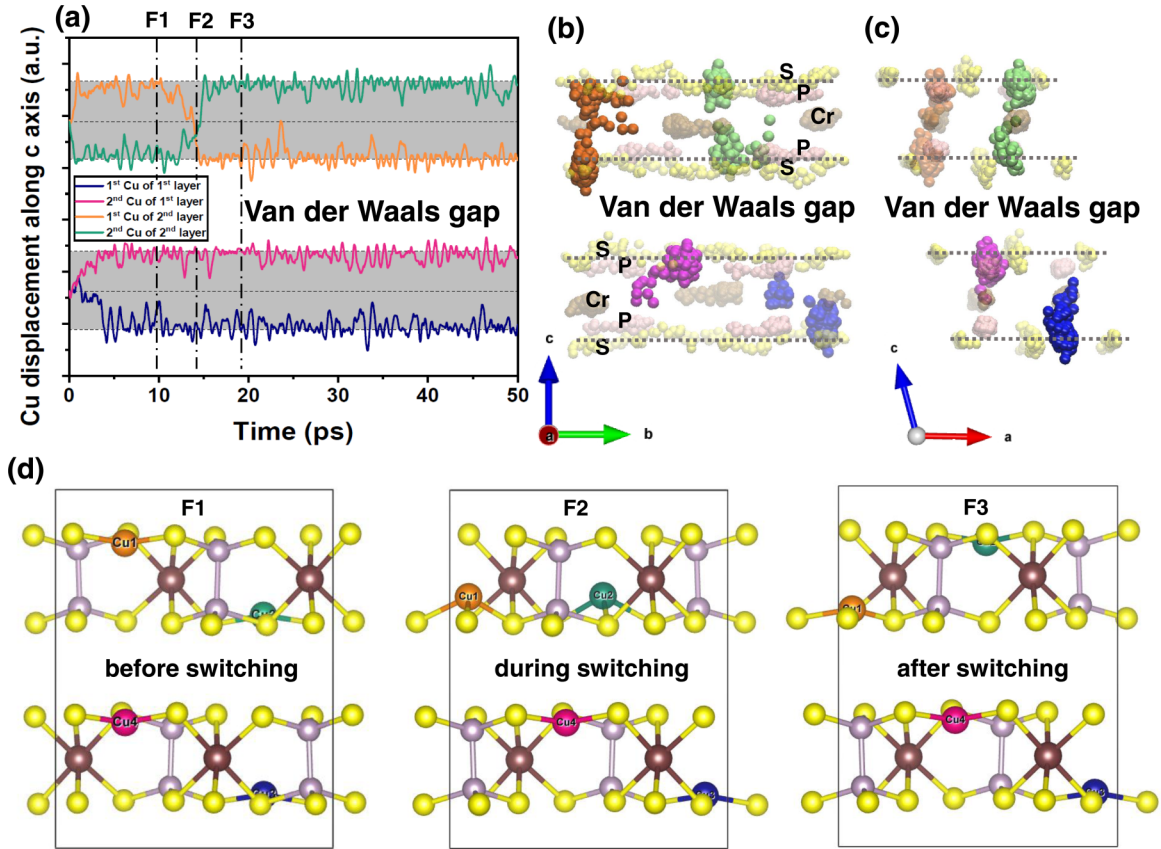


FIG. 6. Quantum molecular dynamics (QMD) simulation to evaluate the trajectory of the antiferroelectric state at 300 K. (a) Displacement of the Cu atoms along the c axis as a function of time. Orange, green colors indicate the displacement of Cu atoms in the first top layer whereas pink and blue colours indicate the same for bottom layer. [(b), (c)] Trajectory of all the atoms for 50 ps in a single frame along a and b . The Cr atoms are shown in the same color as in (a) for a clear understanding. Also P, S, and Cr atoms are made translucent to make the Cr atoms visible. (d) Snapshot of atomic positions of the transition before (F1), during (F2), and after switching (F3).

the potential energy curve. The magnitude of the ferroelectric polarization in the IFE state is found to be 48% larger than the FE state. In addition, by employing Γ_1^+ mode, we have found an energetically stable IAFE state along with previously reported AFE state. Following the same prescription, we have reported a rare example of magnetic polar half-metal CuMnP_2S_6 with ferroelectric like distortion within the metallic state. The next compound in the series is NiCrP_2S_6 . Here, we have found that the FE state is unstable, however, IFE state is stable in the insulating phase with finite polarization. This material has triple-well potential in its uniaxial distortion path along the c axis. Finally, NiMnP_2S_6 shows an insulating to metallic phase transition driven by the polar distortion. However, in this case also IFE state is found to be more stable than FE state with large induced polarization. In all the above systems, we have found strong coupling between magnetic anisotropy and spontaneous polarization. Our calculations have suggested that the reversal of the magnetic anisotropic axis is feasible by switching the direction of the polarization vector.

Quantum molecular dynamic calculations revealed that CuCrP_2S_6 is a stable room-temperature IAFE whereas NiCrP_2S_6 , CuMnP_2S_6 , and NiMnP_2S_6 are stable IFEs. The last two materials are stable room-temperature polar met-

als with ferroelectric like distortion. Interestingly, in case of CuCrP_2S_6 , we have observed that in IAFE state the Cu atoms in top layer switch the relative positions while the Cu atoms in the bottom layer remains at the same position, which can be defined as hybrid inter-intra layer antiferroelectric coupling. It is important to note that in all of these compounds the c parameter of their unit cell changes, which in turn reduces the van der Waals gap between the layers. Similarly, when the vdW corrections modifies c parameter by applying uniaxial compressive strain, we could observe the change in stabilities of these stable FE/FE like states. Also we conclude that the results from both with and without van der Waals corrections can lead to exact results at different strain conditions. Similar results are reported in case of CuInP_2S_6 compound [1]. This property is being well-known character for a piezoelectric material. Hence, these compounds can be further studied and modified for the application in piezoelectric, read-write, and memory devices and also in photovoltaic applications due to their wide-range and tuneable band gaps.

ACKNOWLEDGMENTS

M.J.S is thankful to SRM Institute of Science and Technology, Department of Physics and Nanotechnology,

Kattankulathur, Chennai 603 203, for his fellowship. S.G. acknowledges DST-SERB Core Research Grant, File No. CRG/2018/001728 (2019-2022) for funding the project.

Authors thank High Performance Computing Center, SRM Institute of Science and Technology for providing the computational facility.

-
- [1] J. A. Brehm, S. M. Neumayer, L. Tao, A. O'Hara, M. Chyashavichus, M. A. Susner, M. A. McGuire, S. V. Kalinin, S. Jesse, P. Ganesh *et al.*, *Nat. Mater.* **19**, 43 (2020).
- [2] N. A. Spaldin and M. Fiebig, *Science* **309**, 391 (2005).
- [3] A.-Y. Lu, H. Zhu, J. Xiao, C.-P. Chuu, Y. Han, M.-H. Chiu, C.-C. Cheng, C.-W. Yang, K.-H. Wei, Y. Yang *et al.*, *Nat. Nanotechnol.* **12**, 744 (2017).
- [4] Y. Ji, M. Yang, H. Lin, T. Hou, L. Wang, Y. Li, and S.-T. Lee, *J. Phys. Chem. C* **122**, 3123 (2018).
- [5] X. Yuan, M. Yang, L. Wang, and Y. Li, *Phys. Chem. Chem. Phys.* **19**, 13846 (2017).
- [6] E. Bruyer, D. Di Sante, P. Barone, A. Stroppa, M.-H. Whangbo, and S. Picozzi, *Phys. Rev. B* **94**, 195402 (2016).
- [7] J.-J. Zhang, L. Lin, Y. Zhang, M. Wu, B. I. Yakobson, and S. Dong, *J. Am. Chem. Soc.* **140**, 9768 (2018).
- [8] L. Seixas, A. S. Rodin, A. Carvalho, and A. H. C. Neto, *Phys. Rev. Lett.* **116**, 206803 (2016).
- [9] X. Xu, Y. Wang, F.-T. Huang, K. Du, E. A. Nowadnick, and S.-W. Cheong, *Adv. Funct. Mater.* **30**, 2003623 (2020).
- [10] H. Wang and X. Qian, *2D Materials* **4**, 015042 (2017).
- [11] H. Wang and X. Qian, *Nano Lett.* **17**, 5027 (2017).
- [12] M. Osada and T. Sasaki, *Adv. Mater.* **24**, 210 (2012).
- [13] R. Ramesh and N. A. Spaldin, *Nat. Mater.* **6**, 21 (2007).
- [14] R. Ramesh, *Nature (London)* **461**, 1218 (2009).
- [15] D. Khomskii, *Physics* **2**, 20 (2009).
- [16] Ø. Johansen, V. Risinggård, A. Sudbø, J. Linder, and A. Brataas, *Phys. Rev. Lett.* **122**, 217203 (2019).
- [17] X. Tang and L. Kou, *J. Phys. Chem. Lett.* **10**, 6634 (2019).
- [18] Y. Lai, Z. Song, Y. Wan, M. Xue, C. Wang, Y. Ye, L. Dai, Z. Zhang, W. Yang, H. Du *et al.*, *Nanoscale* **11**, 5163 (2019).
- [19] J. Qi, H. Wang, X. Chen, and X. Qian, *Appl. Phys. Lett.* **113**, 043102 (2018).
- [20] S. M. Neumayer, L. Tao, A. O'Hara, J. Brehm, M. Si, P.-Y. Liao, T. Feng, S. V. Kalinin, P. D. Ye, S. T. Pantelides *et al.*, *Phys. Rev. Appl.* **13**, 064063 (2020).
- [21] B. Lin, A. Chaturvedi, J. Di, L. You, C. Lai, R. Duan, J. Zhou, B. Xu, Z. Chen, P. Song *et al.*, *Nano Energy* **76**, 104972 (2020).
- [22] See Supplemental Material at <http://link.aps.org/supplemental/10.1103/PhysRevMaterials.5.054409> for details.
- [23] P. Hohenberg and W. Kohn, *Phys. Rev.* **136**, B864 (1964).
- [24] G. Kresse and J. Furthmüller, *Comput. Mater. Sci.* **6**, 15 (1996).
- [25] P. E. Blöchl, *Phys. Rev. B* **50**, 17953 (1994).
- [26] J. P. Perdew, K. Burke, and M. Ernzerhof, *Phys. Rev. Lett.* **77**, 3865 (1996).
- [27] S. Nosé, *J. Chem. Phys.* **81**, 511 (1984).
- [28] G. Kresse and J. Hafner, *Phys. Rev. B* **48**, 13115 (1993).
- [29] G. Kresse and J. Hafner, *Phys. Rev. B* **49**, 14251 (1994).
- [30] S. Grimme, S. Ehrlich, and L. Goerigk, *J. Comput. Chem.* **32**, 1456 (2011).
- [31] S. Grimme, J. Antony, S. Ehrlich, and H. Krieg, *J. Chem. Phys.* **132**, 154104 (2010).
- [32] E. Kroumova, M. Aroyo, J. Perez-Mato, S. Ivantchev, J. Igartua, and H. Wondratschek, *J. Appl. Crystallogr.* **34**, 783 (2001).
- [33] A. K. Kirov, M. I. Aroyo, and J. M. Perez-Mato, *J. Appl. Crystallogr.* **36**, 1085 (2003).
- [34] V. Maisonneuve, J. Reau, M. Dong, V. Cajipe, C. Payen, and J. Ravez, *Ferroelectrics* **196**, 257 (1997).
- [35] V. Maisonneuve, C. Payen, and V. Cajipe, *J. Solid State Chem.* **116**, 208 (1995).
- [36] J. Banys, V. Samulionis, V. Cajipe, and Y. Vysochanskii, *Ferroelectrics* **257**, 163 (2001).
- [37] S. Abrahams and E. Keve, *Ferroelectrics* **2**, 129 (1971).
- [38] V. Maisonneuve, V. B. Cajipe, A. Simon, R. Von Der Muhll, and J. Ravez, *Phys. Rev. B* **56**, 10860 (1997).
- [39] S. V. Halilov, A. Y. Perlov, P. M. Oppeneer, A. N. Yaresko, and V. N. Antonov, *Phys. Rev. B* **57**, 9557 (1998).
- [40] M. Fujimoto, *The Physics of Structural Phase Transitions* (Springer Science & Business Media, New York, 2004).
- [41] P. W. Anderson and E. Blount, *Phys. Rev. Lett.* **14**, 217 (1965).
- [42] G. Giovannetti and M. Capone, *Phys. Rev. B* **90**, 195113 (2014).
- [43] S. Ghosh, A. Y. Borisevich, and S. T. Pantelides, *Phys. Rev. Lett.* **119**, 177603 (2017).
- [44] H. Sim and B. G. Kim, *Phys. Rev. B* **89**, 201107(R) (2014).
- [45] M. Meng, Z. Wang, A. Fathima, S. Ghosh, M. Saghayezhian, J. Taylor, R. Jin, Y. Zhu, S. T. Pantelides, J. Zhang *et al.*, *Nat. Commun.* **10**, 5248 (2019).
- [46] D. Puggioni, G. Giovannetti, M. Capone, and J. M. Rondinelli, *Phys. Rev. Lett.* **115**, 087202 (2015).